

# Cosmophysical Factors in the Fluctuation Amplitude Spectrum of Brownian Motion

Alexander V. Kaminsky\* and Simon E. Shnoll†

\*Elfi-tech Ltd., Rekhovot, Israel

†Department of Physics, Moscow State University, Moscow 119992, Russia

†Inst. of Theor. and Experim. Biophysics, Russian Acad. of Sci., Pushchino, Moscow Region, 142290, Russia

†Pushchino State University, Prospect Nauki 3, Pushchino, Moscow Region, 142290, Russia

E-mail: shnoll@mail.ru

Phenomenon of the regular variability of the fine structure of the fluctuation in the amplitude distributions (shapes of related histograms) for the case of Brownian motion was investigated. We took an advantage of the dynamic light scattering method (DLS) to get a stochastically fluctuated signal determined by Brownian motion. Shape of the histograms is most likely to vary, synchronous, in two proximally located independent cells containing Brownian particles. The synchronism persists in the cells distant at 2 m from each other, and positioned meridionally. With a parallel-wise positioning of the cells, high probability of the synchronous variation in the shape of the histograms by local time has been observed. This result meets the previous conclusion about the dependency of histogram shapes (“fluctuation amplitudes” of the spectra of stochastic processes) upon rotation of the Earth.

## 1 Introduction

The works surveyed in [1–3] revealed a determinate variation in the spectra of the fluctuation amplitudes (these are the shapes of the related histograms in the characteristics of the various processes under measurement, ranging from the rates of chemical and biochemical reactions to the noises in gravity-gradient antennae and semiconductor circuits, and to radioactive decay). This paper represents data of a similar study of the process of Brownian motion.

## 2 Subject, materials, and methods

In 2006, we studied variations in the shapes of the histograms obtained from measurements of the fluctuations of the velocity of Brownian motion in an aqueous suspension of ZnO (average particle size:  $5 \mu\text{m}$ ). We obtained proofs of the synchronous variations in the histograms plotted according to the measurement data in independent “generators”, placed on a lab bench.

In 2009, the same experiments were retried using 450-nm polystyrene microspheres (manufactured by Polysciences Inc.) with applying an improved measurement technique. The known method of dynamic light scattering (DLS) [4] was applied to measure the fluctuations of the velocity of Brownian motion. The method is based on the measurement of the fluctuations in coherent light scattering across an ensemble of the moving particles. In practice, a collimated laser beam was passed through a glass cell containing suspension of Brownian particles.

Electromagnetic waves, diffracted on the suspended particles, give a rise to a stochastically fluctuating intensity at the detector plane and corresponding photocurrent

$$i(t) \sim \langle E(t) E(t) \rangle.$$

Here, the angle parentheses denote the average of the rapid optical oscillations. A schematic diagram of the experimental installation is shown in Fig. 1.

We took an advantage of the “backscatter” geometry and a multiple scattering mode in our installation. Two identical optical cells (we refer to these as *Brownian signal generators*) were used. Each cell consisted of a 1-mm-spacing glass cell filled with a suspension, and an optoelectronic unit comprising a laser diode, a photodiode, and a preamplifier. Photo currents  $i_1(t)$  and  $i_2(t)$  of the detector were converted into voltage by trans-impedance amplifiers, whose conversion factor is  $r = 10 \text{ MOhm}$ , then were saved on a PC hard disk following digitization in a 42 KHz 12-digit two-channel analog-to-digital converter. The detectors were differential pin photodiodes by Hamamatsu Co. Ltd. The lasers were single-mode VCSEL structures (wavelength:  $\lambda = 850 \text{ nm}$ ; emission bandwidth:  $\sim 100 \text{ MHz}$ ; radiant energy:  $1 \text{ mW}$ ) manufactured by RayCan. Special steps were taken to exclude potential synchronous interference: the sensors were placed on a vibroisolated table; both lasers and the power supply circuits of the amplifiers were separated and duly filtered. A high-pass filter with cutoff frequency below  $30 \text{ Hz}$  was used in the amplification path to minimize vibration-related synchronous interference.

Fig. 2 shows a segment of photocurrent time series  $i_1(t)$  in one of the Brownian generators. The signal’s shape is typical of persistent signals.

The above autocorrelation function of the signal, for moderately large numerical values of  $\tau$ , is described by an exponent  $C(\tau) = \exp(-q^2 D \tau)$  with die-away time determined by the geometry of the scattering and diffusion coefficient  $D = kT/3\pi\eta d$  (Stokes-Einstein formula), where  $k$  is Boltzmann’s constant,  $T$  is temperature,  $\eta$  is viscosity, and  $d$  is the

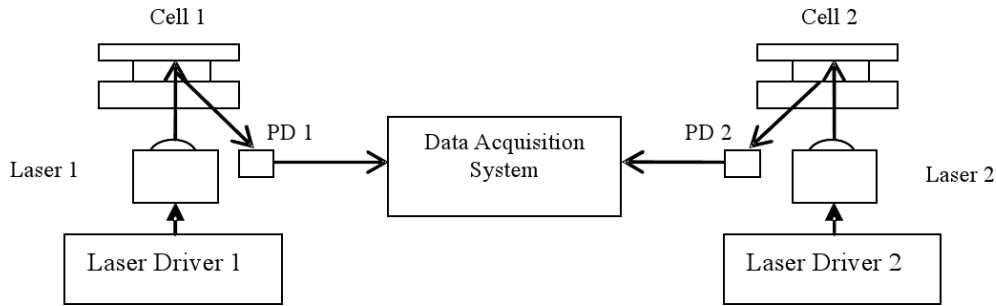


Fig. 1: A schematic diagram of the experimental installation.

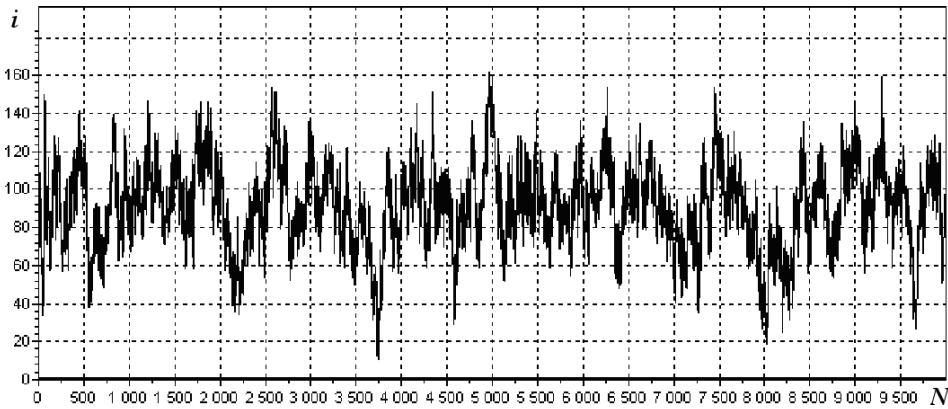


Fig. 2: A segment of time series: a result of DLS signal measurements taken from 1 “generator”: 10,000 measurements of  $1/8,000 = 1.2 \times 10^{-4}$  duration each.

particle’s diameter. The numerical value of  $q$  determines the momentum transfer of a photon in scattering on the Brownian particles. The power spectrum is of Lorentzian-like shape is  $S(\omega) \sim \omega_0/(\omega_0^2 + \omega^2)$ , where  $\omega_0 = 1/T_0$  is the relaxation frequency. With  $\omega \gg \omega_0$ , the spectrum is approximated by a power-law dependence. Similarly, in the time-domain representation, the correlation function may be approximated by the power-law dependence in the area of  $\tau \ll T_0$ .

In our case, the DLS signal is described by a fractional Brownian motion model [5]. The signal is self-similar at the high-frequency range of  $>100$  Hz, and an asymptotic behavior of the correlation function under  $\tau' = q^2 D \tau \rightarrow 0$  is of the power-law nature:  $C(\tau) = 1 - |\tau'|^\alpha$ . Here  $\alpha$  is a scaling parameter related to the fractal dimension  $D = 2 - \frac{1}{2}\alpha$ . At low frequencies we have  $\tau \rightarrow \infty$  and  $C(\tau) = |\tau'|^{-\beta}$ , where  $\beta$  is the scaling parameter related to the Hurst coefficient:  $\beta = 2 - 2H$ .

The following characteristics of the time series were obtained for the DLS signal of the Brownian generators. They are:  $\alpha \approx 0.7$ ,  $D \approx 1.65$ ,  $H = 0.82 \pm 0.1$ .

Fig. 3a shows the autocorrelation function of a signal for one of the channels:  $g_{11} = \langle i_1(t) i_1(t + \tau) \rangle$ , while Fig. 3b shows the cross-correlation function between the channels:  $g_{12} = \langle i_1(t) i_2(t + \tau) \rangle$ .

As seen in 3b, there is no significant physical link between the channels. This might lead to a correlation moment dif-

ferent from 0. Insignificant near-zero-line fluctuations of the cross-correlation function  $g_{12}$  tend to 0 under bigger statistics figures.

### 3 Histogram plotting and shape examination

Amplitude distribution of the histograms were plotted using 30 or 60-measurement series segments. For better convenience of visual comparing, the said histograms were made smooth by the moving summation technique. All the procedures of histogram plotting, smoothing, and scaling were carried out using *Histogram Manager* software developed by Edwin Pozharsky (see [1] for detail).

We consider the histograms to be similar if visual similarity of their shapes can be attained by applying admissible expansion and mirror reflection operations. In other words, the “hystogram shape” can be articulated as an invariant of a subgroup of affine transformations in a plane involving operations of scaling, parallel translation, and  $X$ -axis reflection.

The histogram plotting and shape examination methods are given with requisite particularization used in the studies published in [1].

Fig. 4 shows a chunk of a computer archives: a sequence of the histograms based on the data obtained from the measurements produced in two independent Brownian generators. The histograms were plotted according to the data of

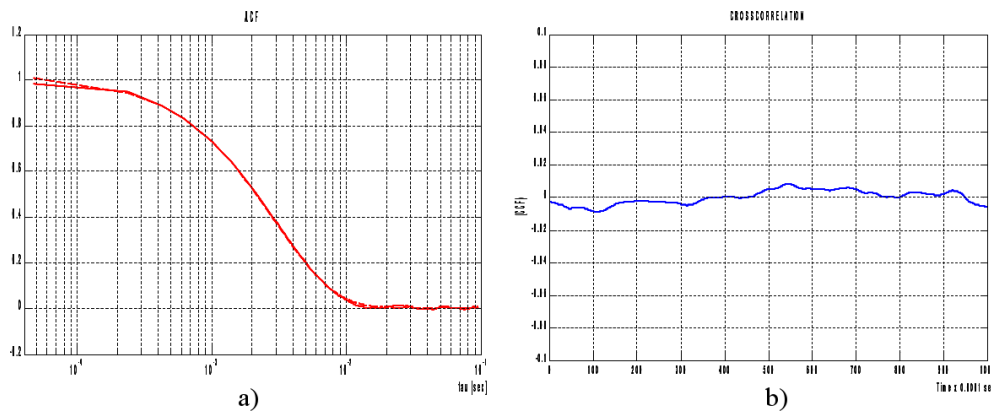


Fig. 3: Autocorrelation (a) and cross-correlation (b) functions for the signals of two “Brownian generators” in our experiment.

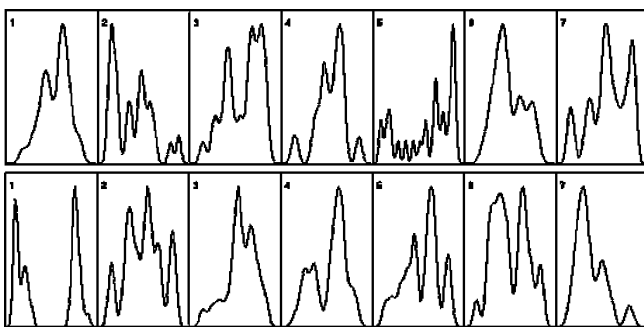


Fig. 4: A chunk of a computer archives: a sequence of the histograms based on the data obtained from the measurements produced in two independent Brownian generators. X-axis in each histogram represents values (in relative units) of the photocurrent in the measurement of Brownian motion. Y-axis gives the number of similar pairs which correspond to the specific values of the photocurrent. The histograms are given after a 17-fold moving-summation smoothing.

30 measurements, and given a 17-fold smoothing. The upper and lower rows show No. 1 and No. 2 generator’s histograms, correspondingly. Numbers of the sequential histograms are shown. The total of the sequential histograms amounted to several thousands.

**4 Synchronous variation of the shape of the histograms in the measurements of Brownian motion on the independent “generators” in the same location**

Fig. 5 shows a chunk of computer archives representing the pairs of *synchronous* histograms plotted on the basis of the data obtained by independent measurements in two installations found to be similar by experts. Numbers of the histograms in the time series are given. As seen in Fig. 5, the synchronous histograms turn out to be similar in shape.

In plotting a distribution of the number of similar pairs of the histograms, according to the values of the related separating intervals, a particularly large number of the similar pairs corresponds to some intervals. This is in exact a core evidence of a non-random nature of the similarity of the his-

Nos. of synchronous histograms in two arrays	$N_1$ (array 1)	$P_1 = \frac{N_1}{720}$	$N_2$ (array 2)	$P_2 = \frac{N_2}{720}$
8	6	0.008	5	0.007
59	1	0.001	3	0.004
232	4	0.006	6	0.008
294	17	0.024	7	0.010
457	2	0.003	13	0.018
		$3 \times 10^{-12}$		$4 \times 10^{-11}$

Table 1: Occurrence frequency of the histograms of the shape under measurements produced in two independent Brownian generators during 24.09.2009 experiment (Fig. 8).

tograms in independent processes.

Fig. 6 shows a distribution of the number of similar pairs of the histograms plotted according to the data obtained by the measurements of Brownian motion in two independent generators.

As seen in Fig. 6, the number of the synchronous pairs is definitely above the “background”. The height of the central log is equal to 89 pairs with 720 histograms in the rows, that is about 12% of the maximumally possible height. In the other intervals, the height of the logs is about 2.5% of the maximumally possible height. Making the use of majorizing estimation by  $\sqrt{N}$  criterion is enough to evaluate the reliability of the inference on the synchronous variation of the histogram shape in independent Brownian generators. The figure shows that the central crest’s height differs from the “background” by around  $6\sqrt{N}$  which corresponds to a  $10^{-11}$  probability for obtaining such a result at random.

It should be noted that according to Fig. 5 the histograms, forming the central log in Fig. 6 and evidencing the synchronous nature of the shape variation of the histograms in independent processes, do not have an apparent difference from the histograms that would correspond to other intervals. In other words, there is no definite shape specifically corresponding to the synchronous variation of the histogram shape.

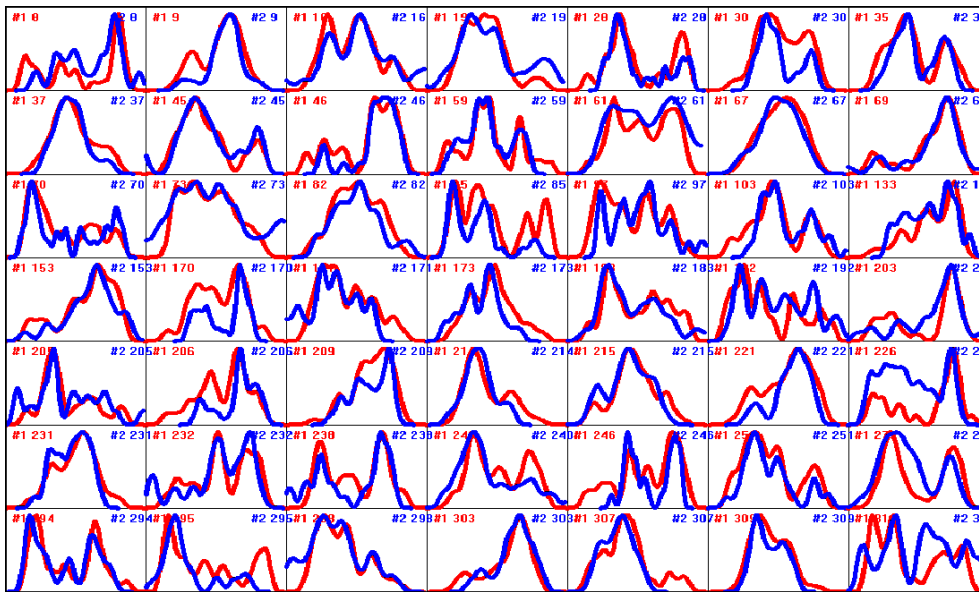


Fig. 5: A log piece: pairs of the histograms plotted on the basis of the data obtained by independent synchronous measurements in two independent Brownian generators found to be similar by an expert evaluation. Numbers of the histograms in the time series are given. Coordinate axes are the same as in Fig. 4.

However, a relatively small number of rare, “exotic” shapes can be found among the histograms that correspond to the central log. The pairs of such histograms that correspond to the central log. The pairs of such histograms can be used for an additional evaluation of the reliability of the core inferences.

At this point, we assume that realization of a complex-shaped histogram is per se an unlikely event to occur. A simultaneous occurrence of rare events in independent measurements is even a less probable event to happen. This evaluation has proven to be very strong. Illustration to this evaluation is given in Fig. 7 and Table 1. Fig. 7 shows 5 pairs of rare-shape histograms obtained synchronously during the 24.09.2009 experiment (there was 89 similar synchronous pairs, all-in-all). We can see, for example, that out of these 720 possible histograms, there was 6 No. 8 histograms in row 1 of the first array, and 5 ones in row 2, thus constituting 0.008 and 0.007 fractions out of the maximal values, respectively.

These fractions do come as an evaluation of the probability of a random occurrence of the given-shape histograms at this particular spot. The general probability of the uncertainty of the inference on a synchronous occurrence of similarly-shaped histograms in two independent rows of measurement is equal to the product of these special-case probabilities. For example, given the 5 rare-shape histograms, this general probability constitutes  $P_1 = 3 \times 10^{-12}$  for the first array, and  $P_2 = 4 \times 10^{-11}$  for the second one, i.e., vanishing small values. It should be noted, however, that the number of the synchronous pairs of the rare-shape histograms is considerably large. Thus, the reliability of the inference on the synchronous occurrence of the similarly-shaped histograms in the independent Brownian generators is proven by these two types of evaluation.

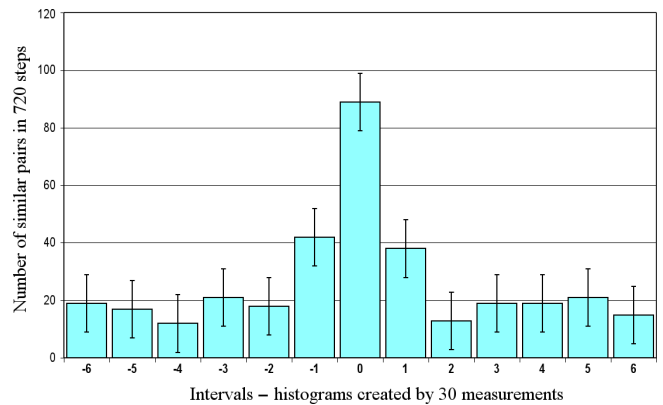


Fig. 6: Shapes of the histograms in the independent Brownian generators vary synchronously. Similar pairs of the histograms are distributed according to the values of the respective separating intervals of time. Date of the experiment: 24.09.2009. Each histogram is plotted according to the data of 30 measurements. X-axis shows values of the time intervals separating similar histograms. One interval is equal to  $3.6 \times 10^{-3}$  seconds.

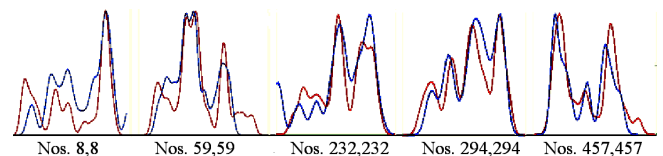


Fig. 7: Examples of the similarity in the rare-shape synchronous histograms according to the occurrence frequency shown in Table 1.

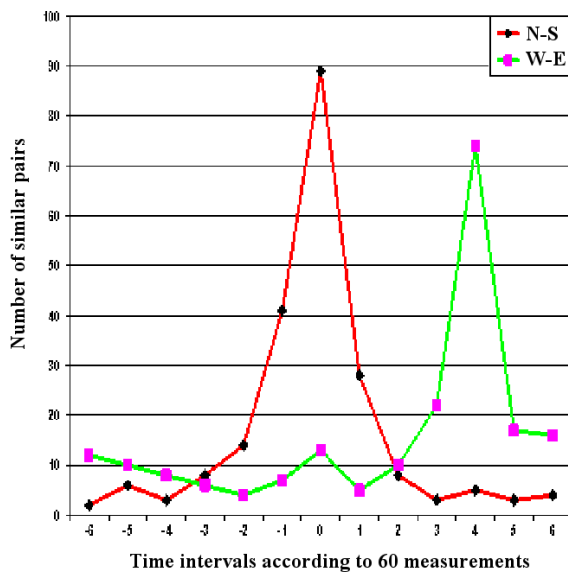


Fig. 8: Interval distribution of the number of similar pairs of the histograms plotted according to the results of 60 measurements produced in two independent Brownian generators which were distant at 200 cm from each other. A) Meridian (from North to South) positioning of the generators; B) Parallel-wise positioning of the generators. In the meridian positioning, the similar histograms occur in the two generators simultaneously. In the parallel-wise positioning, similar histograms of West generator occur 4 interval (11.6 msec) later than they do in the East one.

## 5 Synchronism in different locations

Similarity of the shape of the histograms obtained during independent measurements taken in *different locations at the same local time* comes as an evidence of the dependency of the histogram shape upon rotation of the Earth. Earlier we obtained this evidence by conducting experiments measuring radioactivity at an extremely near distance between the laboratories: at Pustchino (54°N, 37°E) and in Antarctic (Novolazarevskaya Station, 70°S, 11.5°E), so the distance is about 14,000 km. In the works [6–9], when measuring the noise in semiconductor circuits, a “local time effect” was obtained at a distance of about 1 meter. We carried out similar measurements using the “Brownian generators”.

Figs. 8 and 9 show results of the experiments conducted at the town of Rekhovot, Israel (31.89°N, 34.80°E) on October 11, 2009. Two Brownian generators were distant as  $\Delta L = 2$  meters from each other, and were first oriented by the Meridian, then by the Parallel. The signals were recorded for 4 minutes. Local time delay for the said latitude with the basic East-West orientation constitutes  $\Delta T = \Delta L/V$  sec, where  $V \approx 2\pi 6378000 \cos(31.89\pi/180)/86400$  m/sec is the speed of the present point of the Earth’s surface bearing the above specified coordinates. With sampling frequency of 42 KHz, this delay value corresponds to 3.6 histograms plotted by 60 points, and to 7.1 histograms plotted by 30 points. As seen in the drawings below, the time intervals, where the maximal

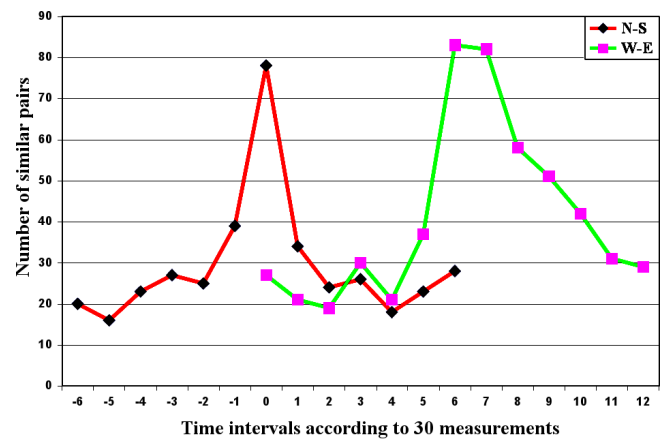


Fig. 9: Interval distribution of the number of similar pairs of the histograms plotted according to the results of 30 measurements produced in two independent Brownian generators at a distance of 200 cm from each other. The local-time synchronism has a more distinct manifestation under the 30-result plotting. In the meridian positioning of the independent generators, similar histograms occur simultaneously. In the parallel-wise positioning, similar histograms of West generator occur in West generator 7–8 intervals later than they do in the East one.

number of the similarly-shaped histograms is found, are close to the estimated values.

## 6 Discussion

Our study of Brownian motion by means of the dynamic light scattering method showed that the fine structure of the distribution of intensity fluctuations of the light, scattered by Brownian particles (shapes of the corresponding histograms) varies synchronously by local time. In other words, Brownian motion is specific for the same regularities as those found previously during examination of stochastic processes of a different nature, namely — those of chemical reactions, thermal fluctuation in resistors, radioactive decay etc. Thus, the similar regularities in the processes, where the energy changing range varies by many orders, show up the same space-time being the only thing in common. Proceeding from this fact, a conclusion was made according to which the observed regularities were explained by the space-time fluctuations determined by the motion of the Earth in a surrounding inhomogeneous gravitational field [1–3].

## Acknowledgements

We are grateful to Prof. P.S. Lande for her valuable discussion and interpretation of the results. Our thanks also come to Head of the Chair of Biophysics of Department of Physics of the Moscow State University Prof. V.A. Tverdislov, and to the workers of the Laboratory of Physical Biochemistry of Institute of Theoretical and Experimental Biophysics of the Russian Academy of Science (Prof. D.P. Kharakoz) for their very valuable discussion. We are tremendously grateful to

Ms. Anna A. Andreyeva for her mission as the second independent expert who compared the histograms in this study.

Submitted on January 21, 2010 / Accepted on February 04, 2010

## References

1. Shnoll S.E. Cosmic physical factors in random processes. Svenska fysikarkivet, Stockholm, 2009, 388 pages.
2. Shnoll S.E. and Rubinstein I.A. Regular changes in the fine structure of histograms revealed in the experiments with collimators which isolate beams of alpha-particles flying at certain directions. *Progress in Physics*, 2009, v.2, 83–95.
3. Shnoll S.E. The “scattering of the results of measurements” of processes of diverse nature is determined by the Earth’s motion in the inhomogeneous space-time continuum. The effect of “half-year palindromes”. *Progress in Physics*, 2009, v. 1, 3–7.
4. Goldburg W.I. Dynamic light scattering. *Am. J. Phys.*, 1999, v. 67, no. 12.
5. Beran J. Statistics for long-memory processes. Chapman & Hall, New York, 1994.
6. Panchelyuga V.A., Kolombet V.A., Pancheluga M.S., and Shnoll S.E. Local-time effect on small space-time scale. In: *Space-Time Structure*, collected papers, Tetru, Moscow, 2006, 344–350.
7. Panchelyuga V.A., Kaminsky A.V., Pancheluga M.S., and Shnoll S.E. Experimental investigation of the existence of a local-time effect on the laboratory scale and the heterogeneity of space-time. *Progress in Physics*, 2007, v. 1, 64–69.
8. Kaminsky A.V., Shnoll S.E. The study of synchronous (by local time) changes of the statistical properties of thermal noise and alpha-activity fluctuations of a 239-Pu sample. arXiv: physics/0605056.
9. Panchelyuga V.A., Kolombet V.A., Kaminsky A.V., Pancheluga M.S., and Shnoll S.E. Local-time effect observed in noise processes. *Bull. of Kaluga University*, 2006, no. 2b, 3–8.